Relationship Between Creep Damage Modes and Creep-fatigue Interaction

K. YAGI, K. KUBO, O. KANEMARU, C. TANAKA and H. MASUDA

National Research Institute for Metals, Tokyo, Japan

ABSTRACT

A predominant creep damage mode resulting in creep fracture is dependent on temperature and stress. Therefore, creep-fatigue interaction must be understood in connection with the relevant creep damage mode. In order to examine the relationship between the creep damage mode and the creep-fatigue interaction, a combined creep-fatigue loading test was carried out for 1Cr-Mo-V, 2.25Cr-1Mo, 304 and 316 stainless steels and Alloy 800H. Creep damage and fatigue damage which were accumulated until rupture were described as a function of linear life fraction damage in addition to a interaction term. The function of creep damage and fatigue damage obtained, which is fracture criterion under creep-fatigue condition, was closely related to each creep damage mode.

KEYWORDS

Creep damage mode ; wedge-type cracking ; creep cavity formation ; creep-fatigue interaction ; combined creep-fatigue loading test.

INTRODUCTION

Cumulative damage under creep-fatigue loading is generally evaluated by linear accumulation damage rule of both creep and fatigue fractions since Taira proposed its concept (Taira, 1962). The damage summation, however, depends on material, temperature, loading condition and so on, and the rule gives either conservative results (Wood, Wynn, Baldwin and O'riordan, 1980) or unconservative ones (Jaske, Mindlin and Perrin, 1973). Predominant creep damage mechanism leading to creep fracture is a function of temperature and stress (Miller and Langdon, 1979). Creep-fatigue life might be affected by the change of creep damage mode. Therefore, the relationship between creep damage mode and creep-fatigue interaction must be investigated.

In the present paper, creep fracture mechanism was first examined for 1Cr-Mo-V steel, 2.25Cr-1Mo steel, 304 and 316 stainless steels and Alloy 800H.

Then combined creep-fatigue loading tests were carried out for these materials under the creep loading condition corresponding to each characteristic creep damage mode observed, in order to clarify the relationship between the creep damage mode and creep-fatigue interaction.

MATERIALS AND EXPERIMENTAL PROCEDURE

The materials tested were 1Cr-Mo-V steel forging for turbine rotor of outside diameter 1160mm, normalized and tempered 2.25Cr-1Mo steel plate of thickness 100mm, 304 stainless steel plate of thickness 21mm, 316 stainless steel plate of thickness 24mm, and Alloy 800H bar of diameter 25mm.

The stress-controlled creep loading and strain-controlled fatigue loading were alternately repeated in the combined creep-fatigue loading test. The loading schedule for the stress and strain, and the hysteresis loops in this test are shown schematically in Fig.1. The combined creep-fatigue loading tests were carried out on servo-hydraulic testing machines with two function generators for creep loading and for fatigue loading (Yagi, Tanaka and Kubo, 1985). The combined creep-fatigue loading test method has four basic parameters of creep stress(σ_c), creep time(t_c), total strain range($\Delta\varepsilon_t$) and number of cycles(N) as shown in Fig.1. The value of σ_c was chosen from creep fracture mechanism map where typical creep damage mode was observed. In the combined creep-fatigue loading test, t_c was 5h and 10h, $\Delta\varepsilon_t$ was 1%, and N was from 2 to 50 cycles. A tensile rate at creep loading and a compressive rate after creep loading were from 15 to 20MPa/s. The strain rate under fatigue loading with a triangular wave form was 10^{-3}1/s.

RESULTS AND DISCUSSIONS

Creep Fracture Mode

In order to chose the creep loading condition for the combined creep-fatigue loading test, the microstructure and fracture surface of the specimens ruptured in the static creep tests were observed, and the creep fracture mechanism map was constructed experimentally.

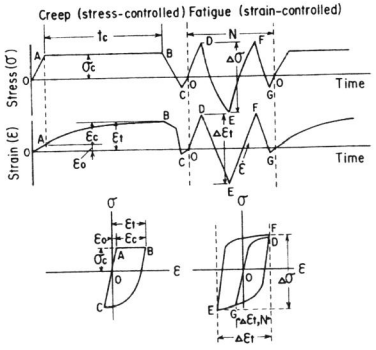

Fig.1. Loading schedule for stress and strain in combined creep-fatigue loading test.

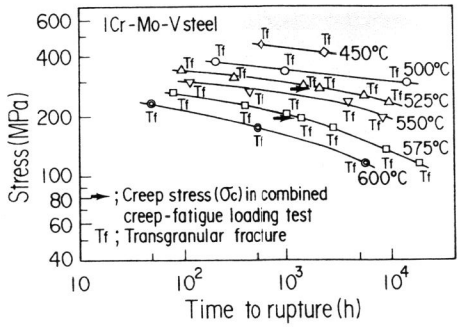

Fig.2. Creep fracture mechanism map for 1Cr-Mo-V steel.

Figure 2 shows the creep fracture mechanism map obtained for 1Cr-Mo-V steel. Only transgranular fracture mode was observed within the range of this experiment. The arrows in this figure represent the creep loading condition (temperature and stress) for the combined creep-fatigue loading test. The creep loading condition for this steel is 274MPa at 525℃ and 196MPa at 575℃, and no formation of creep cavity and crack is expected under these creep loading conditions.

Figure 3 shows the creep fracture mechanism map obtained for 2.25Cr-1Mo steel and the creep loading condition of combined creep-fatigue loading test (147MPa at 550℃). Even for time to rupture over 10^5h, the creep fracture mode was only transgranular, and any cavity and crack were not confirmed.

For 304 and 316 stainless steels, two types of intergranular creep damage, i.e. wedge-type crack and cavity, were observed in addition to the transgranular fracture mode. The wedge-type crack was observed in the specimen ruptured at 550℃ for 316 stainless steel. When this steel is crept at 550℃, the matrix of the steel is hardened by strain aging (Yagi, Tanaka and Kubo, 1985). The intergranular fracture due to wedge-type cracking for this steel seems to be closely related to hardening of the matrix due to strain aging occured during creep. The cavities were observed at the interface between matrix and carbide or sigma phase on the grain boundary.

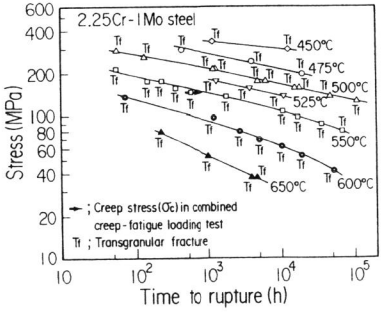

Fig.3. Creep fracture mechanism map for 2.25Cr-1Mo steel.

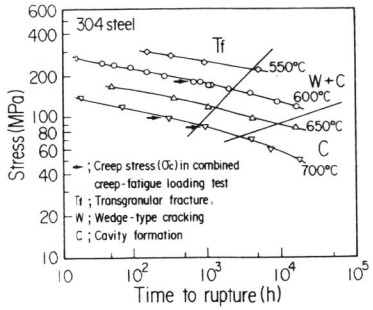

Fig.4. Creep fracture mechanism map for 304 stainless steel.

Figures 4 and 5 show the creep fracture modes summarized from the metallurgical observation of specimens ruptured for 304 and 316 stainless steels, respectively. The arrows in Figs.4 and 5 represent the creep loading condition of combined creep-fatigue loading test for both steels. For 304 stainless steel, the σ_c-values of 176MPa at 600℃ and 98MPa at 700℃ are within the region of transgranular fracture, and the σ_c-value of 86MPa at 700℃ is within the region of intergranular fracture due to mixed intergranular damage mode of cavity formation and wedge-type cracking. For 316 stainless steel, the σ_c-value at 550℃ is 352MPa and corresponds to the region of intergranular fracture due to wedge-type cracking caused by hardening of matrix, the σ_c-values at 650℃ are 167 to 206MPa and within the region of transgranular fracture, and the σ_c-value at 750℃ is 74MPa and corresponds to the region of intergranular fracture due to cavity formation.

Figure 6 shows the creep fracture mechanism map for Alloy 800H obtained from the metallurgical observation of the specimens ruptured. Alloy 800H showed intergranular fracture due to wedge-type cracking except for higher stresses at 600℃. Figure 7 shows the microcracks observed in the specimen ruptured at 750℃. The microcrack was often found at the interface between carbide and precipitation-free zone (PFZ) along the grain boundary and at the interface between precipitated matrix and PFZ. The wedge-type cracks observed by an optical microscope was formed by interlinking of such microcracks. The

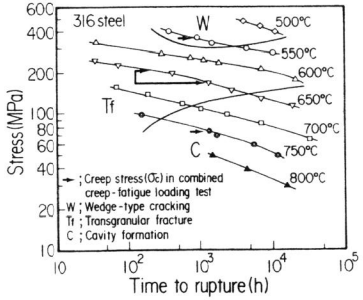

Fig.5. Creep fracture mechanism map for 316 stainless steel.

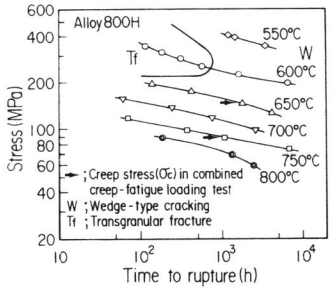

Fig.6. Creep fracture mechanism map for Alloy 800H.

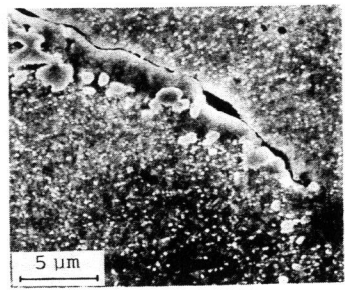

Fig.7. Microcracks observed along grain boundary for Alloy 800H.

wedge-type cracking for Alloy 800H seems to be caused by the discrepancy of relative strength between the grain boundary softened by the formation of PFZ and the matrix hardened by the precipitation of carbide. The creep loading condition of combined creep-fatigue loading test for Alloy 800H corresponds to the region of intergranular fracture due to wedge-type cracking as shown by the arrows in Fig.6.

Fatigue Properties

Fatigue tests were carried out for each testing material at the same temperature as the combined creep-fatigue loading test, in order to obtain basic data which are to be compared with the rupture life and fracture mode of combined creep-fatigue loading test. The strain rate of the triangular wave form in the fatigue test was 10^{-3}1/s. 1Cr-Mo-V and 2.25Cr-1Mo steels were softened under fatigue loading, while 304 and 316 stainless steels and Alloy 800H were hardened under fatigue loading. All specimens in fatigue test were fractured by the transgranular propagation of surface crack.

Relationship between Creep Damage Mode and Creep-Fatigue Interaction

The creep damage, ϕ_c, and fatigue damage, ϕ_f, which were accumulated until rupture of the specimens in the combined creep-fatigue loading tests were calculated using a linear accumulation damage rule (Taira, 1962) as follows :

$$\phi_c = N_c \frac{t_c}{t_R} \tag{1}$$

$$\phi_f = N_c \left(\frac{N-1}{N_f} + \frac{1}{N_{ff}} \right) \tag{2}$$

where N_c is the number of blocks to rupture in the combined creep-fatigue loading test, t_R is the time to rupture in a creep test under the loading condition of σ_c, the value of N_f is the number of cycles to rupture in a fatigue test under the total strain range condition of $\Delta\varepsilon_t$, and N_{ff} is the number of cycles to rupture in the fatigue test at $\Delta\varepsilon_{t,N}$ which is shown in Fig.1. The term $\Delta\varepsilon_{t,N}$ corresponds to the strain range at Nth cycle under fatigue loading in the combined creep-fatigue loading test.

No Intergranular Creep Damage Condition. The combined creep-fatigue loading tests were carried out for each material under the creep loading condition

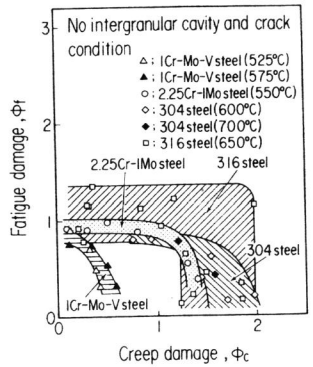

Fig.8. ϕ_c vs. ϕ_f relations for no intergranular cavity and crack condition.

which corresponds to the region of transgranular fracture on the creep fracture mechanism maps shown in Figs.2, 3, 4 and 5. Figure 8 shows the relation of ϕ_c and ϕ_f calculated using the equations (1) and (2). The summation of ϕ_c and ϕ_f is much more than unity in most instances. The rupture life is determined by the accumulation of either creep damage or rupture life is determined by the accumulation of either creep damage or fatigue damage. The ϕ_c vs. ϕ_f relation for 1Cr-Mo-V steel agreed well with the results of creep-fatigue interspersion tests conducted by the Metal Properties Council (Curran and Wundt, 1976).

Wedge-type Cracking Condition. The combined creep-fatigue loading tests were carried out for 316 stainless steel and Alloy 800H under the creep loading condition which is within the region of wedge-type cracking on the maps shown in Figs.5 and 6. Figure 9 shows the ϕ_c vs. ϕ_f relation calculated using Eqs. (1) and (2). The summation of ϕ_c and ϕ_f is much less than unity with a few exceptions. The rupture life under wedge-type cracking condition is strongly affected by creep damage and fatigue damage.

Cavity Formation Condition. Figure 10 shows the ϕ_c vs. ϕ_f relation for 304 and 316 stainless steels in the case of the creep loading condition which

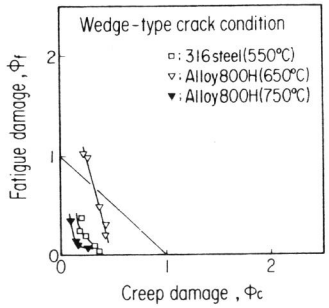

Fig.9. ϕ_c vs. ϕ_f relations for wedge-type crack condition.

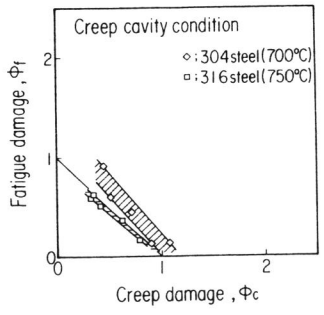

Fig.10. ϕ_c vs. ϕ_f relations for creep cavity condition.

Table 1. Constants of equation (3) estimated.

Materials	(i) Wedge-type cracking			(ii) No intergranular cavity and crack			(iii) Cavity formation		
	Φ_{c0}	Φ_{f0}	α	Φ_{c0}	Φ_{f0}	α	Φ_{c0}	Φ_{f0}	α
1Cr-Mo-V	–	–	–	-0.5	-0.2	-0.76	–	–	–
2.25Cr-1Mo	–	–	–	0.3	-0.1	-0.76	–	–	–
304	–	–	–	0.5 to 1	-0.2	-0.75	0	0	0
316	0	0	2.7	0.3 to 1	0 to 0.3	-0.82	0	0	0
Alloy 800H	0	0	5.9	–	–	–	–	–	–

corresponds to the region of cavity formation on the creep fracture mechanism maps shown in Figs.4 and 5. The summation of ϕ_c and ϕ_f is approximately unity.

The ϕ_c vs. ϕ_f relations were closely related to the creep damage mode as shown in Figs.8, 9 and 10. The simplest function that describes the experimental data can be given by adding a interaction term to the linear accumulation damage rule (Lagneborg and Attermo, 1971 and Wood, 1966) as follows :

$$(\phi_c-\phi_{c0})+\alpha[(\phi_c-\phi_{c0})(\phi_f-\phi_{f0})]^{0.5}+(\phi_f-\phi_{f0}) = 1 \qquad (3)$$

where ϕ_{c0} , ϕ_{f0} and α are constants. The value of ϕ_{c0} , ϕ_{f0} and α was estimated to the lower bound of the ϕ_c vs. ϕ_f relations obtained for each material under each creep damage mode condition. Table 1 shows the value of ϕ_{c0} , ϕ_{f0} and α estimated. For the creep damage mode condition of wedge-type cracking, the value of ϕ_{c0} and ϕ_{f0} are zero, and the value of α is 3 to 6. For no intergranular creep damage condition, the value of ϕ_{f0} is -0.2 to 0.3 and the value of α is about -0.8, both values being independent on the materials tested. The value of ϕ_{c0} , however, is not independent on the materials. The value of ϕ_{c0} for cyclically softened materials is small and the one for cyclically hardened materials is large. The value of ϕ_{c0} is related to hardening or softening of material under fatigue loading. For the creep damage mode condition of cavity formation, the ϕ_{c0} , ϕ_{f0} and α is zero and the linear accumulation damage rule is satisfied.

Life Prediction

It was apparent from the combined creep-fatigue loading test results that the fracture criteria under creep-fatigue condition, i.e. the ϕ_c vs. ϕ_f relations, were closely related to creep damage mode. A procedure for life prediction taking account of variation in the creep damage mode was proposed as shown in Fig.11. This proposed life prediction method is more accurate and reasonable than the conventional method without any consideration of the variation of creep damage mode (Yagi, Kanemaru, Kubo and Tanaka, 1987).

CONCLUSIONS

(1) The ϕ_c vs. ϕ_f relations obtained from combined creep-fatigue loading tests were closely connected with the creep damage mode.
(2) The function which described the fracture criterion under combined creep-fatigue loading, i.e. the ϕ_c vs. ϕ_f relation, was

$$(\phi_c-\phi_{c0})+\alpha[(\phi_c-\phi_{c0})(\phi_f-\phi_{f0})]^{0.5}+(\phi_f-\phi_{f0}) = 1$$

where ϕ_{c0} , ϕ_{f0} and α are constants. The value of these constants depended on

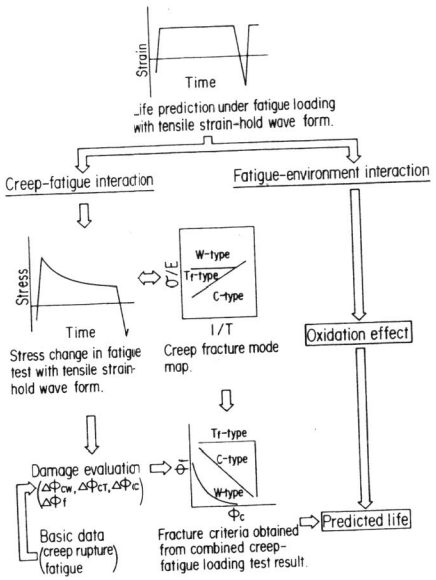

Fig.11. Procedure to predict the life under creep-fatigue conditions.

the relevant creep damage mode.
(3) The life prediction method in which the fracture criteria under creep-fatigue loading were changed according to the variation in creep damage mode was more accurate and reasonable than the conventional method without any consideration of the variation of creep damage mode.

REFERENCES

Curran, R.M. and B.M.Wundt (1976). In: 1976 ASME-MPC Symp. on Creep-Fatigue Interaction (R.M.Curran, ed.), pp.203-282. ASME MPC, New York.

Jaske, C.E., H.Mindlin and J.S.Perrin (1973). Fatigue at Elevated Temperature, ASTM STP 520 (A.E.Carden, A.J.McEvily and C.H.Wells, ed.), pp.365-376. ASTM, Philadelphia.

Lagneborg, R. and R.Attermo (1971). Metall. Trans., 2, 1821-1827.

Miller, D.A. and T.G.Langdon (1979). Metall. Trans. A, 10A, 1635-1641.

Taira, S. (1962). In: Creep in Structure (N.J.Hoff, ed.), pp.96-124. Springer-Verlag, Berlin.

Wood, D.S. (1966). Welding Research Supplement, 45, 90-96.

Wood, D.S., J.Wynn, A.B.Baldvin and P.O'riordan (1980). Fatigue Engng Mater. and Struct., 3, 39-57.

Yagi, K., C.Tanaka and K.Kubo (1985). J. Mater. Testing Res. Assos., 30, 53-59 (in Japanese).

Yagi, K., C.Tanaka and K.Kubo (1985). Trans. ISIJ, 25, 1179-1186.

Yagi, K., O.Kanemaru, K.Kubo and C.Tanaka (1987). Fatigue Fract. Engng Mater. Struct., 9, 395-408.